



**Univerzita Komenského v Bratislave**  
**Fakulta matematiky, fyziky a informatiky**



**Mgr. Jozef Klimo**

**Autoreferát dizertačnej práce**

**Properties and Production Possibilities of Exotic Nuclei**  
**(Vlastnosti a možnosti produkcie exotických jadier)**

**na získanie akademického titulu philosophiae doctor**

**v odbore doktorandského štúdia:**

**4.1.5 Jadrová a subjadrová fyzika**

**Bratislava 2019**

**Dizertačná práca bola vypracovaná v dennej forme doktorandského štúdia  
na Fyzikálnom ústave Slovenskej Akadémie vied**

**Predkladateľ:** Mgr. Jozef Klimo  
Oddelenie jadrovej fyziky  
Fyzikálny ústav Slovenskej akadémie vied  
Dúbravská cesta 9  
Bratislava, 845 11

**Školiteľ:** Mgr. Martin Veselský, PhD.  
Oddelenie jadrovej fyziky  
Fyzikálny ústav Slovenskej akadémie vied  
Dúbravská cesta 9  
Bratislava, 845 11

**Štúdijný odbor:** 4.1.5 Jadrová a subjadrová fyzika

**Predseda odborovej komisie:**

Prof. RNDr. Jozef Masarik, DrSc.  
Fakulta matematiky, fyziky a informatiky UK.  
Mlynská dolina  
Bratislava 842

## Abstrakt

Pomocou sofistikovaných mikroskopických modelov, akými sú Boltzmann-Uehling-Uhlenbeck model (BUU) a Constrained Molecular Dynamics (CoMD) boli študované potlačenia produkčných účinných prierezov super-ťažkých jadier vznikajúcich v reakciách horúcej a studenej fúzie. Z experimentálne získaných pravdepodobnosti vytvorenia zloženého jadra za posledné dekády, boli odvodené ohraničenia pre stavovú rovnicu jadrovej hmoty,  $K_0 = 240 - 260$  MeV a  $\gamma = 0.6 - 1.0$ . Tento výsledok taktiež korešponduje so stavovou rovnicou odvodenou pre nedávno registrovanú zrážku dvoch neutrónových hviezd, tj. udalosť GW170817, potvrdzujúc náš výsledok o stavovej rovnici.

V práci sú študované taktiež jadrové reakcie ako zdroj rádioaktívnych zväzkov. Uvádzané sú simulované kumulatívne účinné prierezy výťažkov spalačných reakcii (ABRABLA07 kód) a hlboko-nepružných zrážok (DIT+SMM kód) použitím moderných modelov jadrových reakcii. Oba reakčné mechanizmy boli podrobené štúdiu pri rôznych energiách zrážok, ako aj kombináciách projektil vs. terč, za účelom zosilnenia produkčných účinných prierezov, a to pre veľké množstvo exotických jadier. Následne vyššie toky rádioaktívnych zväzkov, tak môžu skvalitniť základný aj aplikovaný výskum, a tiež otvoriť nové možnosti v ich napredovaní.

V rámci skvalitňovania teoretických modelov jadrových reakcií je ich konfrontácia s reálnymi dátami nevyhnutná. Len nedávno boli namerané dáta z fragmentačných reakcii experimentu SPALADiN, prostredníctvom ktorých boli analyzované výstupy modelov INCL++, kombinovaného so štatistickými modelmi pre popis de-excitačnej fázy, a to ABLA07, GEMINI++, SMM. Výsledky sú taktiež diskutované v práci.

## Abstract

Fusion hindrance in reactions leading to super-heavy elements via cold and hot fusion is investigated using microscopic model of Boltzmann-Uehling-Uhlenbeck (BUU) and Constrained Molecular Dynamics model extended by quantum-mechanical fluctuations. Density dependent single-particle mean field with isospin dependence is considered. Pauli blocking for protons and neutrons is considered, and Coulomb interactions are introduced. Sensitivity of fusion vs. quasi-fission dynamics on the modulus of incompressibility  $K_0$ , governing competition of surface tension and Coulomb repulsion, and on the density dependence of symmetry energy  $\gamma$ , responsible for formation of neck region, is observed. Experimental fusion probabilities are used to derive constraint on the nuclear equation of state of nuclear matter,  $K_0 = 240 - 260$  MeV and  $\gamma = 0.6 - 1.0$ . These results are in relatively good compliance with constraints derived based on the recently measured data of two neutron stars GW170817.

Along the study of properties of nuclear matter from the point of view of reaction dynamics, this thesis provides calculations for the most promising mechanism for production of exotic nuclei. Cumulative and isotopic cross sections are investigated in spallation and deep-inelastic transfer reactions, performed at wide energy range and various projectile-target combinations using ABRABLA07 model (spallation fragments), and model combination DIT + SMM (deep-inelastic fragments). Appropriate combination of projectile and target, and appropriate incident energy can rapidly improve production cross section of wide range of exotic nuclei and thus, can widely enhance yields of radioactive ion beams more and more frequently used in fundamental and applied research programs.

Prediction powers of theoretical models used for simulation of spallation/fragmentation reaction phase (INCL++) and describing statistical de-excitation (ABLA07, GEMINI++, SMM) are confronted with recently measured SPALADiN experimental data and results are discussed.

## Project of PhD Thesis

This thesis is connected with investigation of production possibilities of exotic nuclei and properties of very isospin asymmetric exotic nuclei, finite nuclear matter. The main tools of this thesis are heavy ion collisions from the Coulomb barrier up to relativistic energies. The subject of the presented PhD thesis can be divided into following parts:

- Investigation of fusion vs. quasi-fission dynamics in the context of nuclear equation of state. Many body approach of following microscopic models is used: the Boltzmann-Uehling-Uhlenbeck model (BUU) and Constrained Molecular Dynamics model (CoMD). It is the first time the experimental fusion probabilities are used to derive constraint on the nuclear equation of state.
- In order to expand the present possibilities of production of radioactive ion beams via spallation reactions, and to investigate a new possibilities using deep-inelastic transfer reactions, simulations using various transport models are presented here. Dependence of production cross section of spallation product on incident proton energy, and spallation of light target materials ( $^{12}\text{C}$ ,  $^{28}\text{Si}$ ,  $^{40}\text{Ca}$ ,  $^{48}\text{Ti}$ ) will be investigating in the present work. Deep-inelastic transfer reactions induced by n-rich exotic nuclei on uranium target  $^{238}\text{U}$  are considered as option for production of a new n-rich nuclei from  $Z = 65$  to  $Z = 70$ . This goal is unattainable by present fragmentation technique but seem to be possible within HIE-ISOLDE post-accelerator facility using deep-inelastic transfer reactions.
- The model of intra-nuclear cascade INCL++ combined with three different statistical models, i.e. ABLA07, GEMINI++ and SMM, are confronted with experimental data from fragmentation reactions in SPALADiN experiment, i.e.  $^{136}\text{Xe} + p$  and  $^{136}\text{Xe} + ^{12}\text{C}$  at 1 AGeV. Drawbacks of models are discussed in the work.

## Introduction

An important goal of heavy ion nuclear physics was achieved by extracting information about properties of nuclear matter at higher and lower densities than saturation density  $\rho_0 \approx 0.16 \text{ fm}^{-3} \approx 3.10^{14} \text{ g/cm}^3$  [Sie87]. The first measurements were possible after the BEVELAC at the Lawrence Laboratory in Berkeley and the Synchrophasotron in Dubna started their operation at the beginning of the seventies of the 20<sup>th</sup> century. These measurements provided relativistic heavy ion collisions, where nuclei were compressed in extremely short time, with typical time scale  $30 \text{ fm}/c = 10^{-22}\text{s}$  [Ber88]. In the nuclear matter experiments, one can usually measure final products created after decompression phase, and reconstruction of history is performed by sophisticated analysis. After many decades of that research, this field still remains one of the most topical with many opened questions related with the explosion mechanisms of supernovae, the interior structure of neutron stars, and initial formation of the universe depending on nuclear matter at wide range of densities and temperatures. Along with experimental data, the theoretical microscopic models represent the main tool in study of equation of state of nuclear matter. The most advanced models sensitive to equation of state of nuclear matter are based on molecular dynamics, incorporating density dependent nuclear mean field, and taking into account dissipation effects. The most successful models designed on those principles are the Improved Quantum-Molecular Dynamics model (ImQMD) or other approximations of Boltzmann equation, such as the Boltzmann-Uehling-Uhlenbeck model (BUU) or the Constrained Molecular Dynamics model (CoMD). Nonetheless, progress on the field of microscopic models is still required and the model parameters should be refined to describe reactions with various isospin asymmetries of interacting nuclei. The significant highlight of nuclear physics is to find universal model capable to describe any type of nuclear collision. Probably the highest level of model universality one can find among models for relativistic collisions.

Nucleus-nucleus collisions along with nucleon-nucleus collisions at intermediate and high

energies are presently at the forefront in production of unstable exotic nuclei and radioactive ion beams. These types of reactions allow spectroscopic measurements of nuclear matter with various isospin asymmetries, and provide answers to complex questions on behavior of atomic nuclei. On the other hand new physical questions are revealed as we go deeper in nuclear theory. It should be mentioned, that a great success on the field of radioactive ion beams came with development of the ISOL (Isotope Separation On-Line) method [Han51]. Use of that technique allows unstable nuclei, formed in the thick target after irradiation by proton beam, to be transported, ionized and subsequently re-accelerated as secondary low energy beams for decay spectroscopy. The worldwide leading facility of that kind is radioactive beam facility ISOLDE (CERN), where around 1000 isotopes of 75 different elements are possible to study by combination of spallation reactions (e.g.  $p + {}^{238}\text{U}$  at 1.0 or 1.4 AGeV) and ISOL technique. Similar effect can be achieved by complementary method of in-flight fragmentation (IFF), usually performed with beryllium target in inverse kinematics. Very advantageous is to use of spallation source as neutron converter. This configuration enables production of approximately 15 neutrons in a single spallation, in average, where subsequently many of them can induce low energy fission with production of n-rich fragments. This is for example not possible using compound nucleus reactions.

Besides spallation and fragmentation reaction mechanism also deep-inelastic transfer reactions seem to be very perspective for future experiments with radioactive ion beams. This reaction mechanism is characterized by intense evolution of isospin degree of freedom, resulting to production of wide range of isotopes characteristic by high transfer of linear and angular momentum. For this mechanisms Fermi energy domain is typical, i.e. 15 - 50 AMeV. Especially, the region of very n-deficient isotopes, below  $Z = 30$ , can be prepared in reaction of  ${}^{86}\text{Kr}$ ,  ${}^{82}\text{Se} + {}^{64}\text{Ni}$  at 25 AMeV, where production cross sections exceeding those from spallation reaction of  $p + {}^{238}\text{U}$  at 1 AGeV. Very promising are deep-inelastic reactions leading to production of n-rich nuclei from neutron closed shells  $N = 20$  ( ${}^{40}\text{Ar} + {}^{238}\text{U}$  at 16 AMeV),  $N = 50$  ( ${}^{86}\text{Kr} + {}^{90}\text{Zr}$  at 8.5 AMeV),  $N = 82$  ( ${}^{136}\text{Xe} + {}^{124}\text{Sn}$  at 7 AMeV) [Ves13]. Moreover, comparisons of simulations with existing data at energies below 10 AMeV indicate that even higher production cross sections can be expected compared to Fermi energy domain [Ves11]. However, in order to join deep-inelastic transfer reactions in production of radioactive ion beams some improvements of experimental techniques are necessary.

## Results and Discussions

### 1 Investigation of fusion hindrance in reactions leading to production of super heavy elements using equation of state of nuclear matter

The heaviest elements were synthesized in cold fusion reactions with Pb or Bi targets, up to  $Z = 112$ , accompanied by emission of one neutron [Hof98]. However, a rapid decrease in production cross sections of SHE to the level of few pb, caused by competition with quasi-fission, eliminates cold fusion reaction for investigation of SHE elements heavier than  $Z = 112$ . Therefore, hot fusion has become preferable on the way to the heaviest SHE systems. The hot fusion mechanism has opened up a possibility to synthesize the elements with atomic numbers 113 – 118, first time applied in FLNR Dubna. Use of heavy actinide targets made of uranium up to californium, bombarded by double magic  ${}^{48}\text{Ca}$  nucleus, has allowed to reach this goal [Oga04-13]. Despite the fact that fusion hindrance is not as strong in hot fusion compared to cold fusion reaction, quasi-fission is still present and remains dominant for  $Z > 112$ . Today it is clear that understanding of quasi fission plays a crucial role on the field of synthesis of new SHE. Therefore comprehension of quasi-fission can allow finding appropriate target vs. projectile combination and set the most appropriate beam energy. Besides synthesis of SHE in laboratory conditions, the main factory for their production in the Universe are still astrophysical objects such as neutron stars. These natural factories use r-process nucleosynthesis for production of SHE, which starts after collision of two neutron stars, i.e. two neutron star mergers. After many years of research, the quasi fission process still remains a topic of fundamental research. The systematic measurements on quasi fission were performed by experimental groups from Dubna [Itk03], Tokai [Nis10] and Canberra [Rie13]. Similar to

complete fusion and nuclear fission, quasi fission was theoretically investigated by the model of di-nuclear system [Ada97], [Ada98], [Gia13], and by the Langevin equation [Zag05-07], [Ari12]. Beside others, models based on the Boltzmann equation, such as ImQMD [Wan02], [Wan13], [Zha08], [Cho14] (approximations of Boltzmann equation) or models based on the time dependent Hartree-Fock theory [Gol09], [Wak14], [Obe14], [Sek16] are frequently used as well.

Within this work the studies on fusion hindrance by utilizing two approximation of Boltzmann equation are presented. The first model is based on the Boltzmann-Uehling-Uhlenbeck (BUU) [Ber88] equation whose results are compared with Constrained Molecular Dynamics (CoMD) [Bon94]. Both of these approaches respect Pauli principle, implemented separately for protons and neutrons, and the Coulomb interaction between protons is included too. Both of models describe the reaction dynamics applying similar physics. However, each of them describes nucleon density, and quantum mechanical fluctuations in a different way and collision integral is established differently as well. Our results show the influence of different parameters of the equation of state of nuclear matter (EOS) on the competition of fusion vs. quasi-fission [Ves16], [Kli19]. We have performed a systematic study on the competition of fusion and quasi fission leading to the production of SHE, and BUU and CoMD simulations were compared with experimental data. The high quality data measured in Dubna, Tokai and Canberra allowed us to find more stringent parameterization for the equation of state of nuclear matter nearby scission point of quasi-fission. The constraint relates with the modulus of incompressibility  $K_0$  of the nuclear equation of state and the density dependence of the symmetry energy  $\gamma$ . For selected investigated reactions around Coulomb barrier, the effect of EOS parameterization should play a role in the region where density gradually drops down from saturation density  $\rho_0$  to zero. Such behavior is typical for surface of the di-nuclear system (DNS) and in the neck region where nucleon density differs from those in the bulk of DNS.

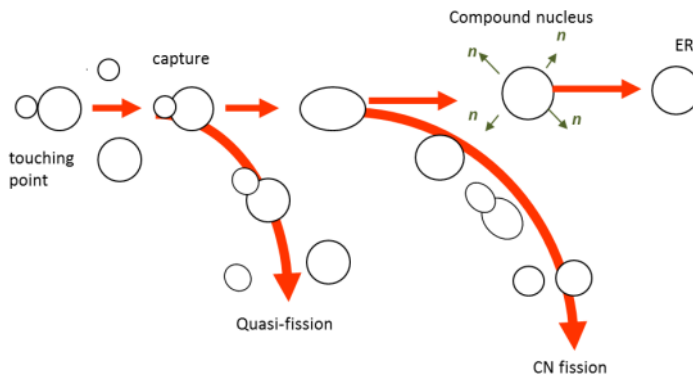


Fig. 1: Central nucleus-nucleus collision: In the first step di-nuclear system is created by capturing projectile nucleus on the target. The created DNS system can evolve to the scission configuration and undergoes quasi-fission or to evolve towards the saddle point of fusion barrier, further evolving to fusion – fission or complete fusion. Then statistical de-excitation takes place.

## 1.1 Constraining of EOS using BUU model

### Assumptions & settings of BUU simulations

In the framework of our simulations we have tested sensitivity of fusion and quasi-fission on various sets of parameters of the equation of state EOS in appropriate set of nuclear reactions leading to formation of SHE. This sensitivity originates from nuclear mean field, which also depends on the energy of symmetry, and is sensitive on  $\kappa(K_0)$  and  $\gamma$  parameters. However, these values are still not exactly known for asymmetric nuclear matter. There are only constraints of these values to certain interval derived from inter-mediate or high energy nucleus-nucleus collisions, collective excitations or from neutron star observation. Therefore, various assumptions on the stiffness of EOS of nuclear matter and assumptions on properties of studied reactions are needed:

- We considered parameter of incompressibility from sufficiently wide range of values, i.e.  $K_0 = 200 - 380$  MeV, also consistent with other measurements, and corresponding to the parameter  $\kappa = 1.16 - 2.0$ . As far as the density dependence of symmetry energy we assumed the interval  $\gamma = 0.5 - 1.5$ .
- The representative set of reactions leading to production of SHE were selected,

where the quality data exist, see the table 1. The collision energy 5 AMeV for each collision in our simulations correspondence to the available data measured experimentally, within few MeV per total beam energy.

- We expected that quasi-fission is dominant at most central collisions with very similar impact parameter, similar as we observe in fusion.
- Due to lack of information on angular momentum of quasi-fission fragments, and in order to eliminate peripheral collisions, we considered only central collisions with impact parameter up to 0.5 fm.
- Time window for observation of each collision was set to  $t = 3\,000$  fm/c. This is long enough to observe fusion or quasi-fission products.
- Each reaction stated in the table 1 were simulated 20 times at a given parameter set  $[K_0, \gamma]$ , using 600 test particles.

By using four Xeon Phi coprocessor cards it was possible to perform many parallel simulations as each of the card is equipped by 61 cores allowing to run up to  $\sim 1\,000$  calculations at once.

Projectile & Target	$P_{CN}$ (exp.)	References
$^{48}\text{Ca} + ^{208}\text{Pb}$	$\sim 1$	[Boc82], [Pro08]
$^{48}\text{Ca} + ^{238}\text{U}$	$\sim 0.2 - 0.5$	[Itk07]
$^{48}\text{Ca} + ^{249}\text{Cf}$	$10^{-3} <$	[Oga12]
$^{64}\text{Ni} + ^{186}\text{W}$	$\sim 0.4 - 0.8$	[Kny08]
$^{64}\text{Ni} + ^{208}\text{Pb}$	$10^{-3} <$	[Boc82]
$^{64}\text{Ni} + ^{238}\text{U}$	$10^{-3} <$	[Koz10]

Tab. 1: Reactions leading to production of SHE, where fusion and quasi-fission was experimentally observed. The set of given reactions we used for testing the sensitivity of DNS system on different EOS.

### **BUU Simulations of nucleonic density**

In our simulations we focused on evolution of nucleonic density within the time window 3 000 fm/c, where each reaction was tested for few parameter sets  $[K_0, \gamma]$ . Based on the evaluated fusion vs. quasi-fission statistics resulting from our simulations, and taking into account the level of compliance with the experimental data, Tab. 1, some of parameter sets  $[K_0, \gamma]$  could be eliminated. Obvious example of interplay between parameter of incompressibility and density dependence of symmetry energy is demonstrated on the figure 2. From all analyzed reactions, the reaction  $^{64}\text{Ni} + ^{186}\text{W}$  shows up as the most sensitive on stiffness or softness of EOS. This is consequence of approximately equal probabilities for fusion and quasi-fission.

One can see, that the choice of soft-soft parameter set  $[K_0, \gamma] = [202 \text{ MeV}, 0.5]$ , caused the system undergoes quasi-fission in all 20 simulated collisions. A splitting of DNS system to two fragments takes place at scission time, typically around 1 200 fm/c. The same scenario was observed in all 20 simulated collisions what imply total disagreement with data. However, we know that it does not correspond to the observed reality, and this parameter set cannot be appropriate, even though our analysis is limited to 20 events.

Since quasi-fission is controlled by counterbalance of surface energy and Coulomb repulsion force, their interplay is deciding. Obviously, the Coulomb repulsion is dominant on the figure 2. In the terminology of EOS, one can say that weak surface tension influences the fusion probability and eventually prevents fusion again quasi-fission. However, to prevent quasi-fission is also possible by controlling the nuclear matter asymmetry in the neck region of DNS. The stiffer the density dependence of symmetry energy the more symmetric content in the neck region one can expect. These statements are demonstrated on the figures 3 and 4, with parameter sets  $[K_0, \gamma] = [300 \text{ MeV}, 0.5]$  and  $[K_0, \gamma] = [202 \text{ MeV}, 1.5]$ , respectively. The figure 3 thus points out on strong stabilization effect of stiff incompressibility as the nucleonic density of DNS is evolving. Even though the density dependence of symmetry energy remains soft, i.e.  $\gamma =$

0.5, the surface tension is sufficient to overcome coulomb repulsion as DNS evolves in time and fusion finally happened. The similar effect can be reached using stiff density dependence of symmetry energy and soft incompressibility parameter, i.e.  $[K_0, \gamma] = [202 \text{ MeV}, 1.5]$ , see the figure 4. In this case, despite the weak surface tension the DNS has more elongated shape, the stabilization is reached, and the system prevents quasi-fission. Hence, softer incompressibility can be compensated by stiffer density dependence of symmetry energy to prolong life time of DNS and fusion is more probable. Eventually, the compound system or mono-nucleus can be formed. This approach of testing EOS parameterization was applied for the rest of reactions. All the results on the constraint of nuclear matter are discussed in the following section.

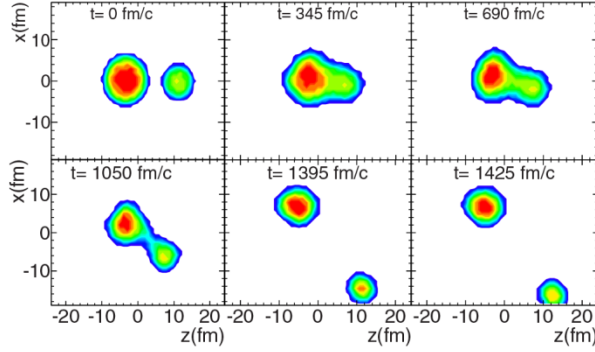


Fig. 2: Evolution of nucleonic density for the most central collisions  $^{64}\text{Ni} + ^{186}\text{W}$  at 5 AMeV. Soft-soft parameter set  $[K_0, \gamma] = [202 \text{ MeV}, 0.5]$  was used.

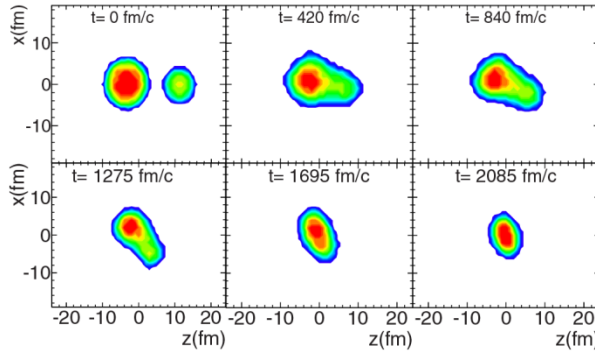


Fig. 3: Evolution of nucleonic density for the most central collisions  $^{64}\text{Ni} + ^{186}\text{W}$  at 5 AMeV. Stiff-soft parameter set  $[K_0, \gamma] = [300 \text{ MeV}, 0.5]$  was used.

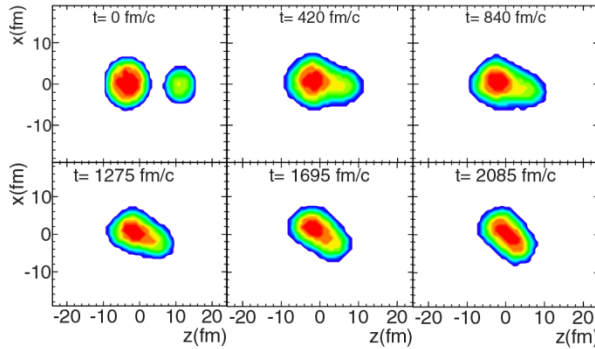


Fig. 4: Evolution of nucleonic density for the most central collisions  $^{64}\text{Ni} + ^{186}\text{W}$  at 5 AMeV. Soft-stiff parameter set  $[K_0, \gamma] = [202 \text{ MeV}, 1.5]$  was used.

### **Constraining the equation of state of nuclear matter using BUU model**

The given set of nuclear reactions can help us to find more stringent constraint of  $K_0$  and  $\gamma$  parameters of EOS. Both of the parameters have impact on nucleonic density evolution as DNS is evolving in time and control competition between quasi-fission and fusion.

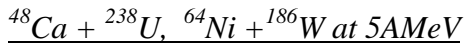
$$\underline{^{48}\text{Ca} + ^{208}\text{Pb}, ^{48}\text{Ca} + ^{249}\text{Cf}, ^{64}\text{Ni} + ^{208}\text{Pb}, ^{64}\text{Ni} + ^{238}\text{U} \text{ at } 5 \text{ AMeV}}$$

(“pure” fusion and “pure” quasi-fission reactions)

Whereas in  $^{48}\text{Ca} + ^{208}\text{Pb}$  reaction fusion is still dominant over quasi-fission, with probability close to  $P_{\text{FUS}} \sim 100$  [%], in collisions  $^{48}\text{Ca} + ^{249}\text{Cf}$ ,  $^{64}\text{Ni} + ^{208}\text{Pb}$ ,  $^{64}\text{Ni} + ^{238}\text{U}$  the fusion probability is strongly hindered. In other words, the probability for the latter set of reactions at the most central collisions can be written as  $P_{\text{FUS}} = N_{\text{FUS}} / N_{\text{TOT}} = N_{\text{FUS}} / N_{\text{QF}} \sim 0$  [%].



Based on our analysis we conclude that any parameterization out of the area  $[K_0, \gamma] = [202 - 230, 0.5 - 1.0]$  results to fusion of the DNS formed in  $^{48}\text{Ca} + ^{208}\text{Pb}$  reaction. However, within that interval quasi-fission became dominant, what is actually in disagreement with the experimental observation, and it incorrectly implies that quasi-fission takes place at mb scale. Therefore, such a soft-soft parameter set can be excluded. The upper constraint we can get from the other three reactions, i.e. pre-dominantly undergo quasi-fission. By investigation of EOS for stiff-soft parameter set  $[K_0, \gamma] = [272 - 300, 0.5 - 1.0]$  we observed too strong stabilization effect on DNS, and fusion became solely dominant channel. Hence, such parameter set does not reproduce the observed reality, and cannot be accepted as well. Also soft-stiff parameterization  $[K_0, \gamma] = [202-255, 1.5]$  leads to dominance of fusion and has to be rejected. In contrast, quasi-fission was observed for  $[K_0, \gamma] = [205 - 255, 0.5 - 1.0]$ . Finally, the presented analysis of almost pure fusion or quasi-fission reactions leads us to constraint of EOS to parameterization  $[K_0, \gamma] = [240 - 255, 0.5 - 1.0]$ . This result is not in contradiction with experimental data for a given set of reactions.



*(fusion and quasi-fission are comparable)*

Based on the previous set of reactions, where fusion or quasi-fission is exclusively dominant, we got constraint on EOS parameters. The given result is reproducing the experimental data well within the sensitivity of method. From the previous simulations we are able to evaluate rough boundaries of  $K_0, \gamma$  region within taken account the sensitivity of that method. Based on the simulation of  $^{48}\text{Ca} + ^{238}\text{U}$  and  $^{64}\text{Ni} + ^{186}\text{W}$  reactions we tried to verified constraint on  $K_0, \gamma$  deduced from the pure fusion or quasi-fission data. The results from both of reactions  $^{48}\text{Ca} + ^{238}\text{U}$  and  $^{64}\text{Ni} + ^{186}\text{W}$  give consistent results with those derived from the reactions where fusion is close to 0 % or 100 %. The constraint on parameterization of EOS was derived from BUU simulations and experimental data to more stringent interval given as  $[K_0, \gamma] = [240 - 260, 0.6 - 1.0]$ , and the 2D plot of possible  $\gamma$  vs.  $K_0$  values is depicted on the figure 5.

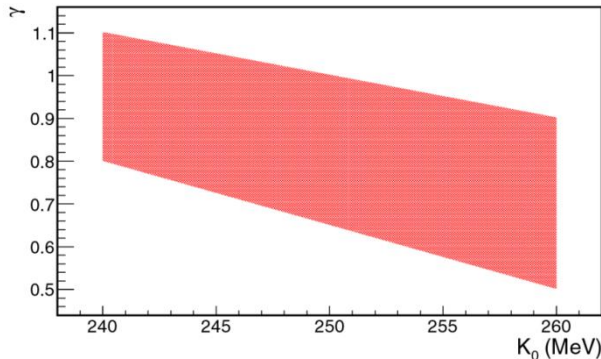


Fig. 5: Constraint on the modulus of incompressibility  $K_0$  describing stiffness of symmetric nuclear matter and on density dependence of the symmetry energy  $\gamma$ . Any parameter set  $[K_0, \gamma]$  used in our simulations from inside of the purple area was in agreement or was not excluded based

## 1.2 Discussion on BUU simulations

The BUU simulations were compared with experimental data and more strict constraint on EOS parameterization was established, ranging within the interval  $K_0 = 240 - 260$  MeV with  $\gamma = 0.6 - 1.0$ , also published in [Ves16]. This implies that DNS system should be driven by stiffer EOS, where maximum density  $1.4 - 1.5$  of the saturation density was reached in the given reactions.

We observed that DNS system typically splits to two fragments at scission time around  $\sim 1300$  fm/c, what seems to be consistent with previous studies with TDHF [Sek16] and ImQMD models [Cho14]. Also the measured kinetic energy of fragments in  $^{64}\text{Ni} + ^{208}\text{Pb}$  and  $^{48}\text{Ca} + ^{238}\text{U}$  reactions is in good agreement with Coulomb potential energy at scission point. As the shell effects are not included in BUU model, fission fragments have symmetric fragment mass distribution. The effect of shell structure is still open question on the field of quasi-fission. Besides shell effects also deformation of target nucleus can impact fusion cross section of SHE.

Whereas deformation can really improve fusion cross section at sub-barrier reactions, its impact on reactions above the Coulomb barrier is still not clear, and its influence cannot be totally excluded. Among others, the recent study on quasi-fission with deformed target nucleus

$^{238}\text{U}$  with  $^{40}\text{Ca}$  above the Coulomb barrier indicates that quasi-fission mass distribution is sensitive on beam energy, and its cross section can be improved with the beam energy [Wak14]. Because the presented constrain on EOS parameterization is relatively narrow, it can imply that if some influence from deformation and shell effects exist, it should not be so significant.

Compared to other methods, e.g. the nuclear giant resonances or nucleus-nucleus collisions at high energies, the method presented here is free of uncertainty related with two body dissipation or by low lying nuclear structure. To go even further and get even more stringent restriction of EOS parameterization more data are demanded, as well improvement of computational power could help significantly.

Even the fact that BUU model offers possibilities to study the EOS, it does not take into account quantum fluctuation. In order to evaluate influence of quantum mechanical fluctuations, we performed equivalent simulations but using another Boltzmann equation approximation as is the CoMD model.

### 1.3 Constraining of EOS using CoMD model

In contrary to BUU simulations, CoMD ones were performed four dimensionally as  $[K_0, \gamma, \text{CSUP}, \sigma_r]$ . Namely,  $K_0$  is incompressibility parameter,  $\gamma$  density dependence of nuclear matter, CSUP is surface energy coefficient from Skyrme potential and  $\sigma_r$  represents width of Gaussian wave packet. In order to successfully describe the quasi-fission for the heaviest DNS systems, the surface term and the nucleonic Gaussian wave packet were optimized within CoMD code together with EOS parameters  $K_0$  and  $\gamma$ . The following set of reactions has been tested:

- $^{48}\text{Ca} + ^{249}\text{Cf}, ^{64}\text{Ni} + ^{208}\text{Pb}, ^{64}\text{Ni} + ^{238}\text{U}$  at 5 A MeV (*“pure” quasi-fission*)
- $^{48}\text{Ca} + ^{208}\text{Pb}, ^{48}\text{Ca} + ^{176}\text{Yb}$  at 5 A MeV (*“pure” fusion*)
- $^{48}\text{Ca} + ^{238}\text{U}, ^{64}\text{Ni} + ^{186}\text{W}$  at 5 A MeV (*fusion and quasi-fission are comparable*)

We paid more attention on the pure quasi-fission systems, and condition to reproduce the fusion data was not considered as strictly. Consequently, the CSUP and  $\sigma_r$  parameters can describe a nucleonic evolution for quasi-fission reactions well, but it results to lower fusion probability for the lighter DNS systems, e.g.  $^{48}\text{Ca} + ^{176}\text{Yb}$ . Also other systems with comparable mass manifest typically lower fusion cross section. Finally, the maximal fusion probability for almost pure fusion reaction has not exceeded more than 30 [%]. Hence, full consensus for both fusion and quasi-fission reactions was not achieved.

Such a discrepancy for pure fusion reaction could be explained by an influence of the Gaussian width on a position of fusion barrier and by surface energy term, which has an direct impact on the single particle mean field. In general, the change of default setting, i.e.  $[\text{CSUP}, \sigma_r] = [-2.0, 1.15]$ , to other combinations leads to instability of compound nucleus CN, as we have observed in reactions with lower mass and atomic number of CN. On the other hand, almost pure quasi-fission DNS systems are reproduced reasonably. Other aspects can relate with the spin-orbital interaction and shell effects, not incorporated in CoMD model [God19].

The systematic CoMD simulations have been performed with the assumption on incompressibility parameter and density dependence of the symmetry energy as the following,  $K_0 = 200 - 290$  MeV (range acceptable by CoMD) and  $\gamma = 0.5 - 1.0$ . And we got the best result for two parameter sets:

- $[K_0, \gamma, \text{CSUP}, \sigma_r]_1 = [245 \text{ MeV}, 0.5-1.0, 0.0 \text{ MeV}/\text{fm}^2, 1.085 \text{ fm}]$
- $[K_0, \gamma, \text{CSUP}, \sigma_r]_2 = [254 \text{ MeV}, 0.5-1.0, -1.0 \text{ MeV}/\text{fm}^2, 1.000 \text{ fm}]$

Only weak influence of density dependence of the symmetry energy was observed on the final fusion and quasi-fission statistics. This conclusion is valid considering the interval  $\gamma = 0.5 - 1.0$ . Thus our observation confirms the similar results on proton induced fission at intermediate energies by CoMD model [Von15], where weak influence of  $\gamma$  on fission was observed for similar interval.

Comparing previous BUU simulations with CoMD ones, we have got comparable constraint. Due to four dimensional simulations, the constraint achieved from CoMD model is not as stringent as we got from BUU. Still, more investigation is needed to distinguished between two possible combinations, i.e.  $[K_0, \gamma, \text{CSUP}, \sigma_r]_1$  and  $[K_0, \gamma, \text{CSUP}, \sigma_r]_2$ .

## 1.4 Discussion on CoMD simulations

In spite of all these differences, the constraint of the incompressibility parameter from CoMD model is consistent with BUU simulations, i.e.  $K_0 = 245 - 254$  MeV [Kli19]. No significant sensitivity of EOS on density dependence of the symmetry energy was observed within the interval  $\gamma = 0.5 - 1.0$ . Neither CoMD nor BUU model considered shell effects or deformed shape of nuclei. However, one can expect that these effects should not influence the entrance channel dynamics and compound system in dramatic way.

In order to verify the two most suitable EOS parameters extracted from CoMD, they have been tested on deep-inelastic transfer reaction of  $^{136}\text{Xe} + ^{198}\text{Pt}$  at 8 AMeV [Wat13]. The CoMD model enables to reproduce these experimental data in principle on the same level as extensively used deep-inelastic transfer model DIT.

Just recently, the simulations of two neutron star mergers point out that at incompressibility of  $K_0 = 245$  MeV [Per19] should lead to formation of neutron star, while the softer EOS parameterization creates conditions for formation of black hole. The simulations were subsequently confirmed in the recent astronomical event GW170817, where a massive neutron star (magnetar) was formed [Abb17], [Per19]. Therefore, one can expect that EOS should be stiffer than softer, resulting from observation of nuclear matter on macro and micro scale.

## 2 Deep-inelastic transfer reactions & HIE - ISOLDE facility

The most of n-rich nuclei from  $Z = 60$  to  $Z = 70$  have been produced in the fragmentation reaction  $^{238}\text{U} + ^9\text{Be}$  at 1 AGeV at FRS facility in GSI, Darmstadt, where isotopic production cross sections varies with few nb [Kur12], [NNDC]. However, the most of nuclei from the given fragmentation mechanism are still relatively close to the line of  $\beta$  stability. In order to get neutron rich nuclei with even higher neutron excess, a new method should be developed.

The deficiency of neutron rich data for  $Z > 60$ , and low production cross sections, can be explained by lower binding energy of neutrons on n-rich side. Therefore, to increase survival probability against neutron emission the excitation energy of nuclei has to be relatively low, especially in the nuclear reaction leading to production of neutron rich radioactive isotopes [Ves13], [Zag11], [Art02]. The very efficient nuclear reaction fulfilling such condition are peripheral nucleus-nucleus reactions of nucleon exchange at the Fermi-energy domain, i.e. 15 - 50 AMeV, [Ves00], [Ves02] [Sou02], [Sou03] or deep-inelastic transfer reactions.

If the impact parameter is sufficient small (0 – 3 fm) central collisions take place, and in order to observed deep-inelastic transfers nuclei have to be approaching each other in semi-peripheral or peripheral collisions. The characteristic interaction time is approximately  $\sim 10^{-21}$ s, depending on incident energy and projectile vs. target combination.

A lot of experimental data have been collected on the many nucleon transfer reaction at the Fermi-energy domain till the present, and very reliable description of experimental data is provided by deep inelastic transfer model of Tassan-Got or DIT [Tas91] (Monte Carlo code). Over the years some modification and enhancement of DIT model were done for Fermi-energy domain and for lower energies as well. In the context of energies below 10 AMeV, the main improvement was done by adjustment of nuclear mean field in the so-called “window“ created in neck region of di-nuclear system (DNS). The “window” allows transfer of nucleons between two parts of DNS, and thus energy and angular momentum can be dissipated [Ves11]. Another enhancement of DIT model is given by incorporation of shell structure, i.e. microscopic effects and thus to consider effect of neutron skin [Ves06]. Many years of development of DIT model results that experimental data are in very good agreement with DIT simulations if the input parameters are handled well, depending on the particular reaction and collision energy.

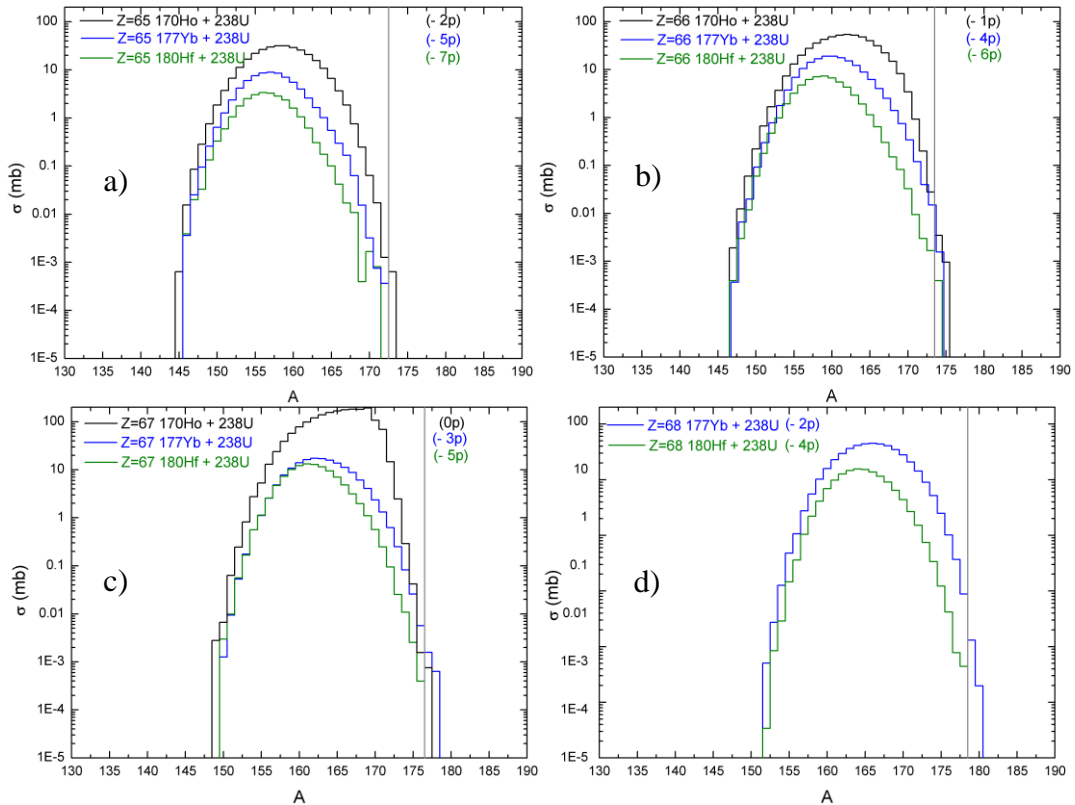
Considering competition of incomplete fusion and pre-equilibrium emission in nucleus-nucleus collisions at the Fermi-energy domain, i.e. following codes can be linked together PE + ICF/DIT + SMM in order to reliable description of experimental data. As for de-excitation phase of reactions, the statistical multi-fragmentation model (SMM code) is very convenient in combination with DIT code.

## 2.1 Cross sections of n-rich nuclei ( $Z = 60 - 72$ ) using DIT + SMM model

The isocaling studies on production cross sections imply that even larger neutron excess in projectile like fragments is achievable by using the projectiles with higher isospin asymmetry [Ves11]. Therefore, we suggest the following reactions  $^{170}\text{Ho} + ^{238}\text{U}$ ,  $^{177}\text{Yb} + ^{238}\text{U}$ ,  $^{180}\text{Hf} + ^{238}\text{U}$  at the energy of post-accelerated beams around 8 AMeV. The radioactive ion beams (RIBs) were chosen with respect on their intensity (2016). The present status of the HIE-ISOLDE facility is that the Phase 2 (energy upgrade) of its upgrade has reached completion in 2018. This allows accelerating exotic nuclei up to 10 AMeV, and after completion of the Phase 3 it will reach even higher intensities. Thus HIE-ISOLDE facility will be only one in the world capable of accelerating medium and heavy radioactive isotopes in this energy range [Kad17], [Kad18].

Because the excitation energy of projectile like fragments typically do not exceed 1 AMeV below incident energy of 10 AMeV, no pre-equilibrium emission can be expected. Thus the model framework can reduce to shorten version, i.e. ICF/DIT + SMM. This combination of codes was eventually utilized to predict production cross sections, with parameterization similar to those used in the previous studies [Ves11]. Particularly, the maximum full density radius  $R_0$  was enlarged by 0.525 fm and the inverse slope of the linear density tail was extended from 0.65 to 1.8125 fm. Each combination projectile and target was performed for 5 million events of peripheral collisions, and after de-excitation by SMM code the residual cross sections were finally evaluated.

Production cross sections are one up to three orders of magnitude higher than those measured by Kurcewicz et al. in the fragmentation  $^9\text{Be} + ^{238}\text{U}$  (1 AGeV) [Kur12], [NNDC], see the Tab. 2. However, this is definitely valid only for some n-rich isotopes, as the fragmentation with Be target allows to investigate more n-rich nuclei in total. In the Kurcewicz experiment, production cross sections were measured from Neodymium to Platinum. These comparisons lead us to the conclusion that deep-inelastic transfers can be opened with significantly higher cross sections as were observed in the fragmentation  $^9\text{Be} + ^{238}\text{U}$  (1 AGeV). The mass distributions and cross sections, see the figure 6 a) – f), with few possible new isotopes were evaluated for the future ISOL type experiments.



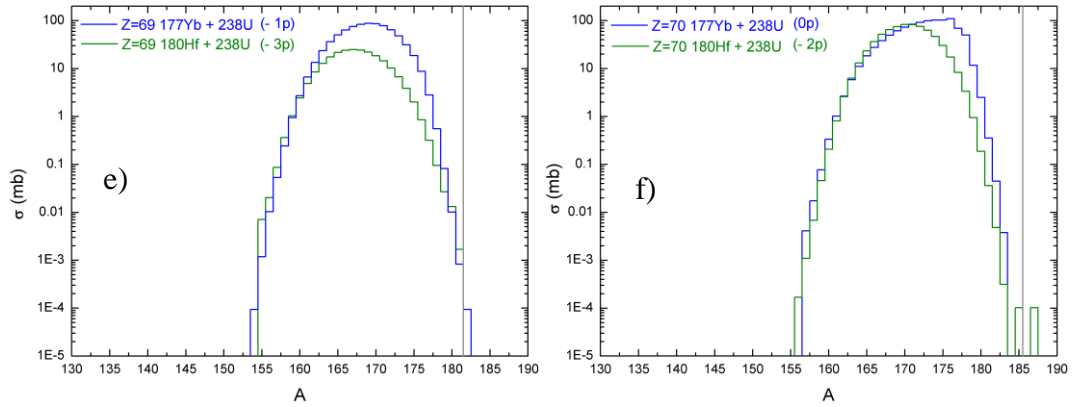


Fig. 6 a) – f): DIT + SMM simulations of production cross sections for elements  $Z = 65 - 70$  produced in the deep-inelastic transfer reactions:  $^{170}\text{Ho} + ^{238}\text{U}$  (black line),  $^{177}\text{Yb} + ^{238}\text{U}$  (blue line),  $^{180}\text{Hf} + ^{238}\text{U}$  (green line). All the reactions were calculated at the collision energy 8 AMeV. On the right side from the gray vertical line the isotopes with no available experimental data are distinguished.

## 2.2 Discussion on DIT+ SMM simulations

In the present work three deep-inelastic transfer reactions are suggested to improve production cross sections of nuclei with atomic numbers  $Z = 65 - 70$ :  $^{170}\text{Ho} + ^{238}\text{U}$ ,  $^{177}\text{Yb} + ^{238}\text{U}$ ,  $^{180}\text{Hf} + ^{238}\text{U}$  at 8 AMeV. The simulations performed using transport model DIT and statistical model SMM indicate that to more than 13 new isotopes ( $Z = 65 - 70$ ) can be produced with production cross sections varies from 0.1 to 10  $\mu\text{b}$ . Post-accelerator of new generation already installed at ISOLDE facility enables to re-accelerate low energy radioactive ion beams coming from spallation target up to 10 AMeV. Thus this goal can be achieved by secondary beams  $^{170}\text{Ho}$ ,  $^{177}\text{Yb}$  and  $^{180}\text{Hf}$  at available intensities  $\sim 10^6 \mu\text{C}$ . From experimental point of view, very sensitive technique has to be applied for complete identification of transfer products. This could be possible with ISOLDE Solenoidal Spectrometer (ISS) capable of complete identification A, Z of transfer products, and measurement of reaction kinematics and Q values. The simulations presented in this work can be used for experiments with n-rich exotic nuclei using secondary deep-inelastic transfer reactions, and may provide guidance for real experiments in the future.

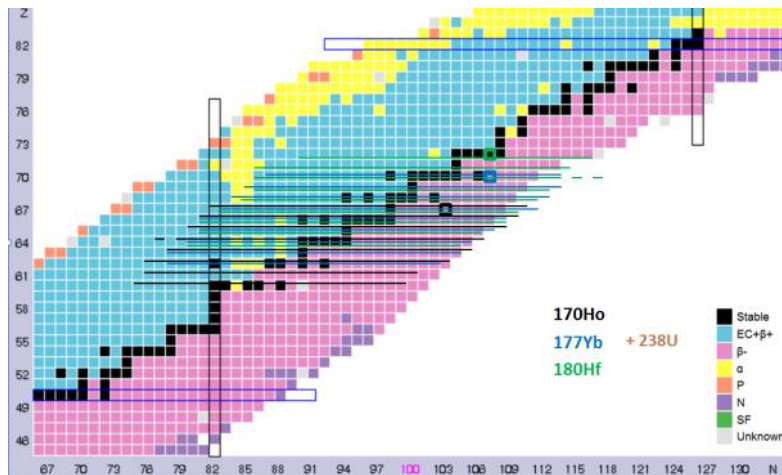


Fig. 7: DIT + SMM simulations: the area of PLF products from  $^{170}\text{Ho} + ^{238}\text{U}$  (black lines),  $^{177}\text{Yb} + ^{238}\text{U}$  (blue lines),  $^{180}\text{Hf} + ^{238}\text{U}$  (green /lines) at the collision energy of 8 AMeV. Some new isotopes from

## 3 Spallation & HIE-ISOLDE facility

### 3.1 Incident energy of protons vs. cross section of spallation products

The reaction of spallation allows us to measure and observe many exotic nuclei with high statistics by advanced ISOL technique. Energy of protons plays a crucial role in collisions where

beams of protons are colliding with a massive uranium target in ISOLDE target station. Further increase of the energy of protons from 1.4 AGeV to 2.0 AGeV can provide not only higher production cross section for available radioactive beams, but can open new possibilities for new isotopic beams, and for secondary post-accelerated beams. These assumptions were investigated via ABRABLA07 simulations. A comprehensive description of the latest version of the code ABLA07 (de-excitation code) [Kel09] is discussed in the IAEA report [IAE08] as well.

ABRABLA07 simulations show that production cross section of intermediate mass fragments (IMF), produced in spallation-fragmentation channel, can increase with higher incident energy, see the figures 8. For spallation-fragmentation at incident energy of 2.0 AGeV one can expect gain factor 2.43 compared to 1.4 AGeV proton collisions, as one can see from the figure 9. This reaction channel allows to produce nuclei from  $Z = 3$  to  $Z = 86$ . The effect of higher proton collision energy on spallation-fragmentation channel can be also seen on the figure 10 a).

On the other hand, spallation-evaporation is dominant at the interval  $Z = 75 - 92$ . This interval is becoming even narrower at 2.0 AGeV. Descending trend of cross section at this energy was observed at  $Z = 85-92$ , and on the other hand it can be improved on the interval  $Z = 72-85$ . This is also the case of Tl isotopes. See the figure 10 b). The total gain in cross section of heavy fragments produced in fragmentation and evaporation at 2.0 AGeV leads to gain of approximately 1.32.

While excitation energy of pre-fragments has the most significant impact on evaporation and fragmentation, it is an angular momentum which has the strongest influence on fission process. Therefore, any stagnation or decrease of spallation-fission cross section with increasing collision energy will affect fission branching ratio, where downward trend is visible from the figure 8.

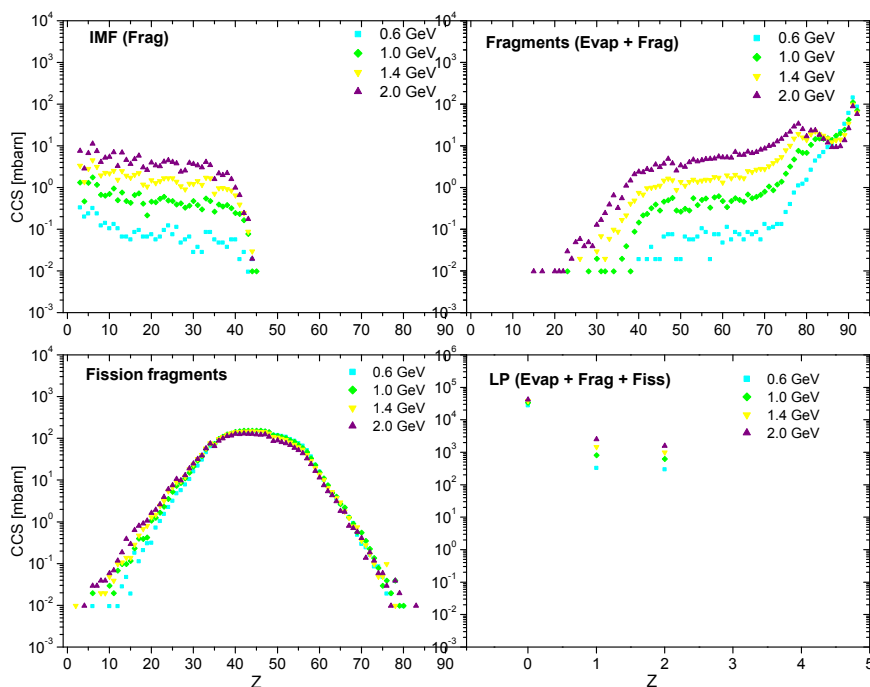
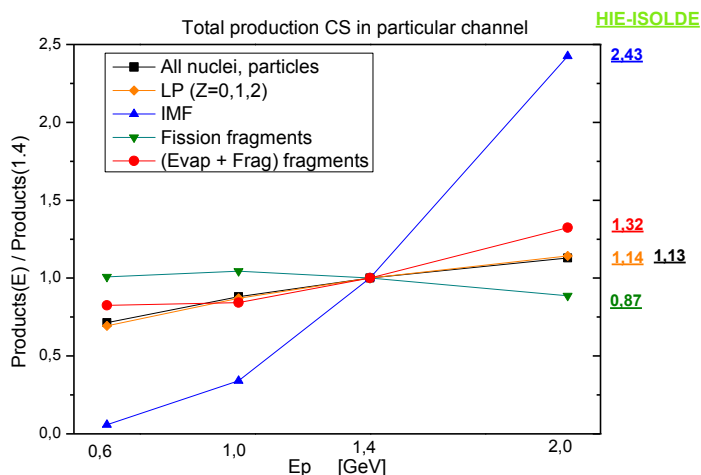


Fig. 8: Cumulative cross sections of recoils from reaction  $p + {}^{238}\text{U}$  at 0.6, 1.0, 1.4, and 2.0 AGeV.

Fig. 9: Comparisons of total cross section for particular de-excitation channel at collision energies of 0.6, 1.0, 1.4, and 2.0 AGeV, normalized to cross sections at 1.4 AGeV.



HIE-ISOLDE

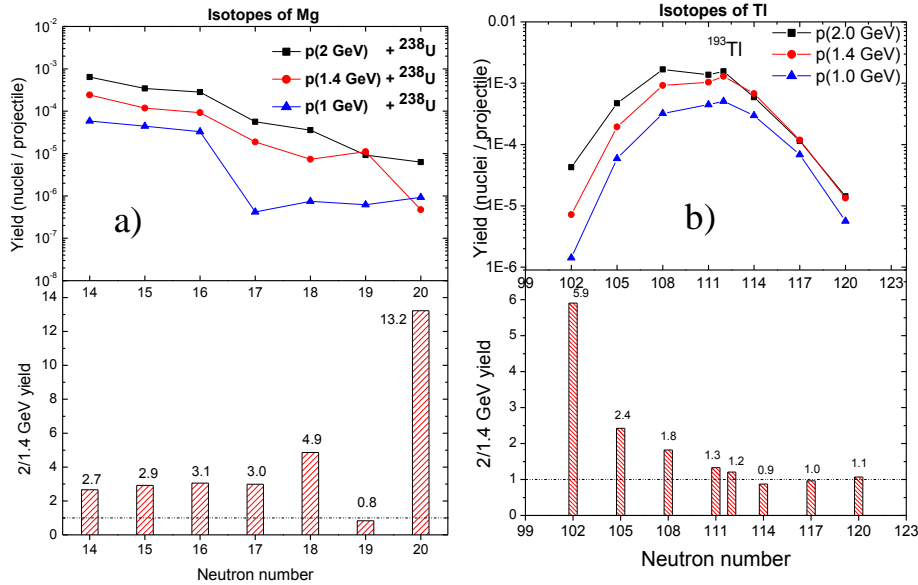


Fig. 10: Yields of n-rich a) Mg and n-deficient b) Tl isotopes in spallation:  $p + {}^{238}\text{U}$  at 1.0, 1.4 and 2.0 AGeV.

### 3.2 Spallation of light targets ${}^{12}\text{C}$ , ${}^{28}\text{Si}$ , ${}^{40}\text{Ca}$ , ${}^{48}\text{Ti}$

In order to produce light isotopes at higher production cross section in spallation and to produce isotopes even closer to proton drip line, the use of light targets could be alternative to heavy actinides targets. We have investigated the spallation of 1.4 AGeV protons on following targets:  ${}^{12}\text{C}$ ,  ${}^{28}\text{Si}$ ,  ${}^{40}\text{Ca}$  and  ${}^{48}\text{Ti}$ , the figure 11. These target elements can be used in ISOLDE experiments where high flux of n-deficient radioactive ion beam, especially light isotope beams is required. The conclusion of spallation simulations of light targets is that spallation-evaporation and spallation-fragmentation are channels contributing to production of any possible fragments. The total production gain for fragments is of one order of magnitude compared to standard uranium target  ${}^{238}\text{U}(\text{Cx})$ . Thus light targets can open up possibilities to make experiments with light radioactive ion beams more time effective, and thus more experiments can be performed at ISOLDE facility within annual schedule. For elements of oxygen, magnesium or argon one can expect following gains of cumulative cross sections compared to standard  ${}^{238}\text{U}$  based target:

- O  $\sim 17x$ , produced in reaction: 1.4 AGeV proton +  ${}^{28}\text{Si}$
- Mg  $\sim 38x$ , produced in reaction: 1.4 AGeV proton +  ${}^{28}\text{Si}$
- Ar  $\sim 48x$ , produced in reaction: 1.4 AGeV proton +  ${}^{48}\text{Ti}$

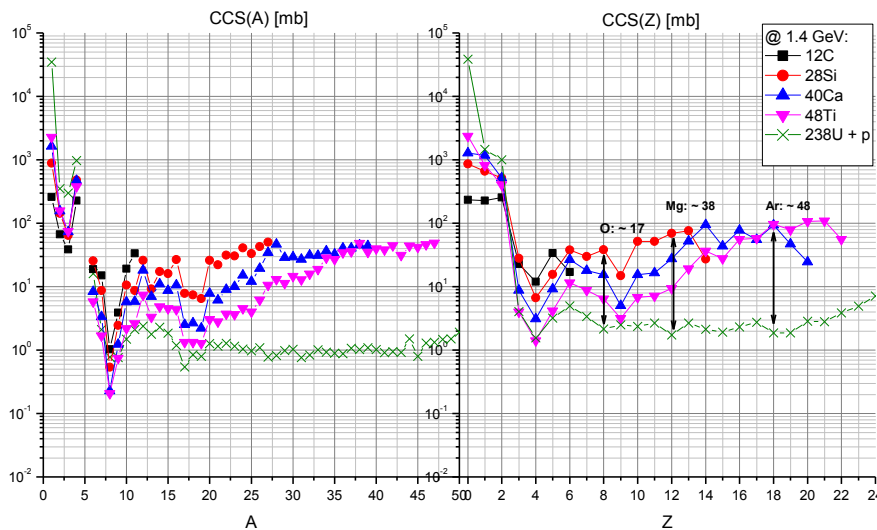


Fig. 11: Comparison of A, Z distributions at proton energy of 1.4 AGeV on light and heavy mass target material.

### 3.3 Discussion on ABRABLA07 simulations

An influence of incident energy of proton on cumulative production cumulative cross sections of n-rich and n-deficient isotopes were investigated on standard ISOLDE target, made of  $^{238}\text{U}(\text{Cx})$  using the Monte Carlo code ABRABLA07. It was shown that increase of proton incident energy from 1.4 AGeV to 2 AGeV can improve fragments production capability of uranium targets, mainly for light and heavy fragments arisen in spallation-fragmentation, and n-deficient heavy fragments produced via spallation-evaporation, mainly out of the fission fragment region. The higher proton energy does not necessarily lead to enhancement in spallation-fission production cross section.

Isotopic cross section of many isotopes of Mg, Ca, Zn, Tl, Pb, Bi, At and Ra have been investigated and discussed at various incident energies within the same model framework of ABRABLA07.

The possibly enhancement of production cross section of light fragments  $Z < 22$  (Ti) was examined in proton induced spallation reactions of few light isotopic targets  $^{12}\text{C}$ ,  $^{28}\text{Si}$ ,  $^{40}\text{Ca}$  and  $^{48}\text{Ti}$ . The simulated cross sections were compared with standard uranium target. That results point to gain in cumulative production cross sections for elements such as O, Mg and Ar in one order of magnitude at least. Thus isotopes belonging to the so-called “Island of inversion”, e.g. some n-rich isotopes of Li, Na, Mg, Si and Ca, are possible to study with better statistics by ISOL methods using light spallation targets.

## 4 SPALADiN experiment, $^{136}\text{Xe} + \text{p}$ and $^{136}\text{Xe} + ^{12}\text{C}$ at 1AGeV

One of the main aims of the presented SPALADiN experiment was to test the two-step hypothesis of nuclear reactions and measure the contribution of different pre-fragment decay channels in the reactions  $^{136}\text{Xe} + \text{p}$  (hydrogen target), and  $^{136}\text{Xe} + ^{12}\text{C}$  (carbon foil) at the energy of 1 AGeV [Gor19]. Both of the reactions have been measured in inverse kinematics at SPALADiN setup in GSI, Darmstadt. The big-aperture dipole magnet together with large acceptance detectors of SPALADiN setup allows to measure final state of charged particles and projectile residue with  $Z \geq 2$  in coincidence with neutrons. Such coincident event-by-event measurement permits to estimate the excitation energy of pre-fragments and to analyze their de-excitation channels. Based on the measured data the elemental production cross sections were compared with existing data and theoretical models. Besides these characteristics, the total multiplicity and the fragment production cross section depending on the excitation energy were studied and models were confronted with measurement.

### 4.1 Measured elemental production cross sections

The production cross sections in SPALADiN experiment in both of reactions were measured from two independent data sets, i.e. we rely on the identification by Time-of-Flight detection system (TOF) in case of lighter charges and by ionization chamber “Forward MUSIC” (FM) used for larger charges. The cross section as a function of  $Z$  is shown on the figure 12 a) and b), for  $^{136}\text{Xe} + \text{p}$  and  $^{136}\text{Xe} + ^{12}\text{C}$  at 1 AGeV, respectively. First of all, one can see the good agreement between data collected from TOF and FM detection system in the overlap region. These overlaps are positioned within  $Z = 23 - 26$ , the collision with hydrogen target, and within  $Z = 12 - 29$  for spallation on the  $^{12}\text{C}$  target, what indicates the proper calibration both of independent detection systems.

Based on the comparison on the figure 12 a), the SPALADiN data agrees with those from FRS experiment, measured by group of Napolitani et al. [Nap07] below  $Z = 6$  and above  $Z = 30$ . Discrepancy is mostly evident in the interval of  $Z = 8 - 26$ , where FRS data are above SPALADiN one. The explanation for such variance is not clear for us. On the other hand, looking at the data measured in direct kinematics and different identification technique provided by Kotov et al. [Kot95], one can see relatively good agreement with SPALADiN experiment. Due to direct kinematics measurement of Kotov, the heaviest elements were not registered, only light inter-mediate mass fragments (IMF). The acceptance correction and correction for detection efficiency in SPALADiN experiment is handled well, as TOF and FM cross sections



are overlapping in IMF fragments region. Therefore, Kotov and SPALADiN data appear more trustworthy in the region of IMF's.

From the comparison of elemental production cross sections on the graphs 12 b) for the second reaction  $^{136}\text{Xe} + ^{12}\text{C}$ , SPALADiN data vs. data of Binns et al. [Bin87] results systematic shift of about 30 %. This shift is more or less constant over whole Z interval. In spite of bit different beam energies in experiments, it could not lead to 30 % shift in cross sections as its dependence on the beam energy around 1AGeV is really small, for quantitative explanations see the figure 9. The most probable explanation of cross section shift is different target thickness for SPALADiN and experiment performed by group of Binns as the target used in the latter experiment was three times thicker. However, this explanation should be verified by another spallation experiment with  $^{136}\text{Xe}$  on with hydrogen target.

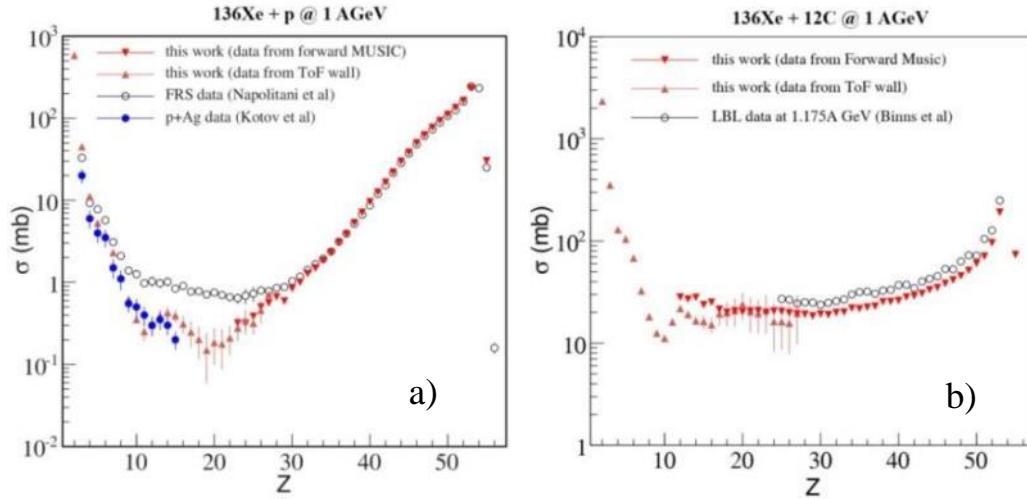


Fig. 12: Elemental production cross sections: a)  $^{136}\text{Xe} + p$  at 1AGeV b)  $^{136}\text{Xe} + ^{12}\text{C}$  at 1AGeV. Experimental data measured in SPALADiN experiment shown by red.

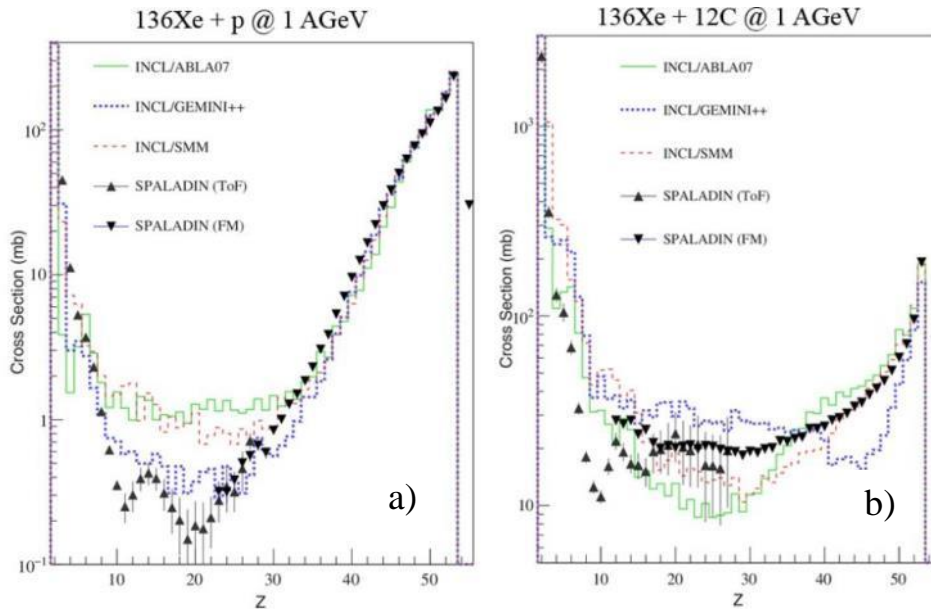


Fig. 13: Elemental production cross sections of reaction: a)  $^{136}\text{Xe} + p$  at 1AGeV and b)  $^{136}\text{Xe} + ^{12}\text{C}$  at 1AGeV. SPALADiN experimental data by black compared with simulations by INCL++ inter-nuclear cascade model in combination with three different de-excitation models ABLA07 (green), GEMINI++ (blue), SMM (red).

## 4.2 Comparison of experimental SPALADiN data with models

In the framework of the comparison of experimental SPALADiN data with our simulations we used only INCL++ as very reliable cascade model in pair with one of three statistical de-excitation models: ABLA07, GEMINI++ and SMM. The collision energy range for INCL++ to work properly was established as 0.15 – 3.0 AGeV, with assumption that following particles or ions are used as impinging projectiles: nucleons, pions, and light ions up to  $A = 18$ . More info related with INCL model could be found in [IAE08] [Bou02]. These collision simulations served us as event generator for GEANT4 simulations where whole SPALADiN setup is included. In orders to compare experimental and modeled data the total cross sections were normalized.

The light fragment ( $Z < 25$ ) from the reaction  $^{136}\text{Xe} + ^{12}\text{C}$  were identified for the first time [Gor19]. Heavier fragment data from this reaction and data from the reaction  $^{136}\text{Xe} + p$  have already existed and were compared with available data. SPALADiN data are also confronted with theoretical models. Intra-nuclear cascade model INCL++ is combined with one of the three statistical models for calculation of de-excitation phase, i.e. ABLA07, GEMINI++ and SMM. A good agreement of INCL++ in a pair with given statistical models was observed for fragments  $Z > 30$  in the reaction  $^{136}\text{Xe} + p$ . Cumulative cross sections for intermediate mass fragments, mainly with  $Z = 10 - 30$ , are reproduced reliably only by GEMINI++ and other two models are in better compliance with the data measured by Napolitani et al. [Nap07]. On the other hand, such a level of agreement between models and SPALADiN data was not achieved in the second reaction  $^{136}\text{Xe} + ^{12}\text{C}$ . In this case, SMM model can only describe experimental data of heavier fragments,  $Z > 40$ , and at lower atomic numbers one can see significant discrepancies. ABLA07 and GEMINI++ provide less reliable results over whole range of atomic numbers.

## 4.3 Discussion on SPALADiN experiment

The given fragmentation reactions  $^{136}\text{Xe} + p$  and  $^{136}\text{Xe} + ^{12}\text{C}$  at 1 AGeV have been studied in inverse kinematics using large-acceptance detectors of SPALADiN setup, in GSI Darmstadt. A big-aperture dipole magnet in combination with large-acceptance detectors enables to measure coincidences of final-state charged particles and fragments ( $Z \geq 2$ ) and neutrons. This allowed that inter-mediate mass fragments from  $^{136}\text{Xe} + ^{12}\text{C}$  have been measured for the first time. Excitation energies of pre-fragments were estimated, and multiplicity of neutrons as a function of excitation energy and atomic number of pre-fragments was studied as well. The cumulative or elemental production cross sections were compared with available data and theoretical models.

Based on the complex analysis of measured data and comparison with intra-nuclear cascade model INCL++ combined with three statistical de-excitation models ABLA07, GEMINI++ and SMM, we conclude that some model improvements are necessary for all used statistical models. However, this task is beyond the scope of this thesis. Some enhancement is requested also for INCL++ model, as we observed discrepancies related with low neutron multiplicity for pre-fragments with lower excitation energy. From the analysis of experimental data from SPALADiN experiment and simulations as well, evaporation de-excitation channel is still dominant, what was confirmed in both reactions.

## Publications in refereed articles

1. **Constraining the equation of state of nuclear matter from competition of fusion and quasi-fission in the reactions leading to production of the superheavy elements**  
M. Veselsky, J. Klimo, Yu-Gang Ma, G. A. Souliotis  
Phys. Rev. C. **94**, 064608 (2016).
2. **Simulation of fusion and quasi-fission in nuclear reactions leading to production of superheavy elements using the Constrained Molecular Dynamics model**  
J. Klimo, M. Veselsky, G. A. Souliotis, A. Bonasera

Nucl. Phys. A **992**, 121640 (2019).

3. **Study of the reaction mechanisms of  $^{136}\text{Xe} + \text{p}$  and  $^{136}\text{Xe} + ^{12}\text{C}$  at 1 AGeV with inverse kinematics and large-acceptance detectors**  
Thomas Gorbinet, Orlin Yordanov, Jean-Eric Ducret, Thomas Aumann, Yassid Ayyad, Sébastien Bianchin, Olga Borodina, Alain Boudard, Christoph Caesar, Enrique Casarejos, Bronislav Czech, Stanislav Hlavac, Jozef Klimo, Nikolaus Kurz, Christoph Langer, Tudy Le Bleis, Sylvie Leray, Jerzy Lukasik, Davide Mancusi, Piotr Pawlowski, Stéphane Pietri, Christopher Rappold, Marie-Delphine Salsac, Haik Simon, and Martin Veselsky  
Eur. Phys. J. A **55**, 11 (2019).
4. **New systematic features in the neutron-deficient Au isotopes**  
M. Venhart, J. L. Wood, M. Sedlák, M. Balogh, M. Bírová, A. J. Boston, T. E. Cocolios, L. J. Harkness-Brennan, R-D Herzberg, L. Holub, D. T. Joss, D. S. Judson, J. Kliman, J. Klimo, L. Krupa, J. Lušnák, L. Makhathini, V. Matoušek, Š. Motyčák, R. D. Page, A. Patel, K. Petrik, A. V. Podshibyakin, P. M. Prajapati, A. M. Rodin, A. Špaček, R. Urban, C. Unsworth and M. Veselský  
J. Phys. G: Nucl. Part. Phys. **44**, 074003 (2017).
5. **Identification of a 6.6 $\mu\text{s}$  isomeric state in  $^{175}\text{Ir}$**   
S. A. Gillespie, A. N. Andreyev, M. Al Monthery, C. J. Barton, S. Antalic, K. Auranen, H. Badran, D. Cox, J. G. Cubiss, D. O' Donnell, T. Grahn, P. T. Greenlees, A. Herzan, E. Higgins, R. Julin, S. Juutinen, J. Klimo, J. Konki, M. Leino, M. Mallaburn, J. Pakarinen, P. Papadakis, J. Partanen, P. M. Prajapati, P. Rahkila, M. Sandzelius, C. Scholey, J. Sorri, S. Stolze, R. Urban, J. Uusitalo, M. Venhart, and F. Weaving  
Phys. Rev. C **99**, 064310 (2019).

#### Other publications

1. **Opportunities for nuclear reaction studies at future facilities**  
Martin Veselsky, Jozef Klimo, Nikoleta Vujisicova and Georgios A. Souliotis  
Conference Istros 2015, arXiv:1604.01961
2. **Direct measurement of fission barrier height of unstable heavy nuclei at ISOL facilities**  
J. Klimo, M. Veselský, R. Raabe, A. N. Andreyev, M. Huyse, P. Van Duppen, F. Renzi, K. Nishio, H. Makii, I. Nishinaka, S. Chiba, G. Souliotis, T. Grahn, P. T. Greenlees, J. Pakarinen, P. Rahkila, M. Venhart, J. Kliman, S. Hlavac, V. Matousek, L. Krupa, I. Sivacek, D. Klac, M. Sedlak, E. Rapisarda, the ACTAR TPC Collaboration  
Proceedings of the HNPS2018, the 27th Annual Symposium of the Hellenic Nuclear Physics Society
3. **EoS studies in nucleus-nucleus collisions: from Coulomb barrier to LHC**  
M. Veselsky, J. Klimo, G. A. Souliotis, X. G. Deng, Y. G. Ma, M. Ploskon  
Proceedings of the 4<sup>th</sup> Workshop on New Aspects and Perspectives in Nuclear Physics, May 5-6, 2017 - Ioannina, Greece

## Bibliography

- [Abb17] B. P. Abbott et al., Phys. Rev. Lett. 119, 161101 (2017).  
 [Ada97] G. G. Adamian et al., Nucl. Phys. A 618, 176 (1997).  
 [Ada97] G. G. Adamian et al., Nucl. Phys. A 627, 361 (1997).  
 [Ada98] G. G. Adamian et al., Nucl. Phys. A 633, 409 (1998).  
 [Ari12] Y. Aritomoet et al., Phys. Rev. C 85, 044614 (2012).  
 [Art02] A. G. Arthuk et al., Nucl. Phys. A 701, 96c-99c (2002).  
 [Ber88] G. F. Bertsch et al., Phys. Rep. 160, No. 4, 189-233 (1988).  
 [Bin87] W.R. Binns et al., Phys. Rev. C 36, 1870 (1987).  
 [Ble99] M. Bleicher et al., J. Phys. G: Nucl. Part. Phys. 25, 1859 (1999).  
 [Boc82] R. Bocket et al., Nucl. Phys. A 388, 334 (1982).  
 [Boh39] N. Bohr et al., Phys. Rev. 56, 426 (1939).

- [Bon94] A. Bonasera, Phys. Rep. 243, 1-124 (1994).
- [Bou02] A. Boudard et al., Phys. Rev. C 66, 044615 (2002).
- [Cho14] R. K. Choudhury et al., Phys. Lett. B 731, 168 (2014).
- [Gia13] G. Giardina et al., Nucl. Sci. Tech. 24, 050519 (2013).
- [God19] K. Godbey et al., arXiv:1906.07623v1.
- [Gol09] C. Golabek et al., Phys. Rev. Lett. 103, 042701 (2009).
- [Gor19] T. Gorbinet et al., Eur. Phys. J. A 55, 11 (2019).
- [Han51] O. Kofoed-Hansen et al., Phys. Rev. 82, 96 (1951).
- [Hof98] S. Hofmann, Rep. Prog. Phys. 61, 639 (1998).
- [IAE08] <https://www-nds.iaea.org/publications/indc/indc-nds-0530/>  
 Proceedings of the Advanced Workshop on Model Codes for Spallation Reactions, ICTP Trieste, Italy, 4-8 February 2008. D. Filges et al., IAEA INDC(NDS)-530, Vienna, August 2008.
- [Itk03] M.G. Itkis et al., Yad. Fiz. 66, 1154 (2003), Phys. At. Nucl. 66, 1118 (2003).
- [Itk07] M. G. Itkis et al., Nucl. Phys. A787, 150 (2007).
- [Kad17] Y. Kadi et al., Proceedings of IPAC2017, Copenhagen, Denmark.
- [Kad18] Y. Kadi et al., CERN Yellow Reports: Monographs, Vol 1 (2018), CERN-2018-002-M.
- [Kel09] A. Kelic et al., arXiv:0906.4193.
- [Kli19] J. Klimo et al., Nucl. Phys. A 992, 121640 (2019).
- [Kny08] G. N. Knyazheva et al., PEPAN Lett. 5, 40 (2008).
- [Kot95] A.A. Kotov et al., Nucl. Phys. A 583, 575 (1995).
- [Koz10] E. M. Kozulin et al., Phys. Lett. B 686, 227(2010).
- [Kur12] J. Kurcewicz et al., Phys. Lett. B 717, 371-375 (2012).
- [Nap07] P. Napolitani et al., Phys. Rev. C 76, 064609 (2007).
- [Nis10] K. Nishio et al., Phys. Rev. C 82, 044604 (2010).
- [NNDC] <https://www.nndc.bnl.gov/>
- [Pro08] E. Prokhorova et al., Nucl. Phys. A 802, 45 (2008).
- [Obe14] V. E. Oberacker et al., Phys. Rev. C 90, 054605 (2014).
- [Oga04] Y.T. Oganessian et al., Phys. Rev. C 69, 054607 (2004).
- [oga04] Y.T. Oganessian et al., Phys. Rev. C 70, 064609 (2004).
- [Nun15] J. Alcántara-Núñez et al., Phys. Rev. C 92, 054602 (2015).
- [Oga06] Y.T. Oganessian et al., Phys. Rev. C 74, 044602 (2006).
- [Oga07] Y.T. Oganessian et al., Phys. Rev. C 76, 011601 (R) (2007)
- [Oga12] Y.T. Oganessian et al., Phys. Rev. Lett. 109, 162501 (2012).
- [Oga13] Y.T. Oganessian et al., Phys. Rev. C 87, 014302 (2013).
- [Oga13] Y.T. Oganessian et al., Phys. Rev. C 87, 054621 (2013).
- [Per19] A. Pergo et al., arXiv:190307898.
- [Rie13] R. du Rietz et al., Phys. Rev. C 88, 054618 (2013).
- [Sek16] K. Sekizawa et al., Phys. Rev. C 93, 054616 (2016).
- [Sou02] G.A. Souliotis, et al., Phys. Lett. B 543, 163 (2002).
- [Sou03] G.A. Souliotis, et al., Phys. Rev. Lett. 91, 022701 (2003).
- [Tas91] L. Tassan-Got et al., Nucl. Phys. A 524, 121-140 (1991).
- [Ves00] M. Veselsky, et al., Phys. Rev. C 62, 064613 (2000).
- [Ves02] M. Veselsky, Nucl. Phys. A 705, 193 (2002).
- [Ves06] M. Veselsky et al., Nucl. Phys. A 765, 252-261 (2006).
- [Ves11] M. Veselsky et al., Nucl. Phys. A 872, 1-12 (2011).
- [Ves13] M. Veselsky, Acta Physica Slovaca, vol. 63, no. 1&2, Nuclear reactions with heavy ion beams.
- [Ves16] M. Veselsky et al., Phys. Rev. C 94, 064608 (2016).
- [Von15] N. Vonta et al., Phys. Rev. C 92, 024616 (2015).
- [Wak14] A. Wakhle et al., Phys. Rev. Lett. 113, 182502 (2014).
- [Wan02] N. Wang et al., Phys. Rev. C 65, 064608 (2002).
- [Wan13] N. Wang et al., Nucl. Sci. Tech. 24, 050520 (2013).
- [Wat13] Y. X. Watanabe et al., Nucl. Instr. Meth. B 317, 752 (2013).
- [Zag05] V. Zagrebaev et al., J. Phys. G 31, 825 (2005).
- [Zag07] V. Zagrebaev et al., J. Phys. G 34, 1 (2007).
- [Zag07] V. Zagrebaev et al., J. Phys. G 34, 2265 (2007).
- [Zag11] V. I. Zagrebaev et al., Phys. Rev. C 83, 044618 (2011).
- [Zha08] F. S. Zhanget et al., Nucl. Phys. A 802, 91 (2008).